Available online at www.sciencedirect.com
SCIENCE DIRECT®
Journal of Power Sources 124 (2003) 432–439
JOURNAL OF POWER SOURCES
www.elsevier.com/locate/jpowsour

Water gas shift reaction kinetics and reactor modeling for fuel cell grade hydrogen

Yongtaek Choi, Harvey G. Stenger*
Department of Chemical Engineering, Lehigh University, Bethlehem, PA 18015, USA

Received 31 March 2003; accepted 25 April 2003

Abstract

The kinetics of the water gas shift reaction was studied to evaluate existing reaction mechanisms, test various rate expressions and simulate the performance in a methanol fuel processor for fuel cell applications. The reaction was carried out in a micro reactor testing unit using a commercial Sud-Chemie $Cu/ZnO/Al_2O_3$ catalyst between 120 and 250 °C with a range of feed rates and compositions. Using non-linear least squares optimization, the parameters in five rate expressions were fit to the experimental data. Based on a review of published work on the WGS reaction mechanism, our study found that a rate expression derived from a regenerative mechanism and another rate expression derived from adsorptive mechanism fit the experimental data equally well. Numerical integration of a one-dimensional PFR model was used for this parameter fitting. An empirical rate expression, $r_{CO} = kP_{CO}P_{H_2O}(1-\beta)$ with activation energy of 47.4 kJ/mol was also obtained from the experimental data. Reactor performance was simulated to determine catalyst loadings required to achieve specific CO conversions as a function of temperature and water feed rate. These results are useful in studying the design trade offs available to reformer systems.

Keywords: Water gas shift; Fuel processing; Methanol steam reforming; Fuel cell; Hydrogen; Reformer

1. Introduction

The water gas shift reaction, used to reduce carbon monoxide in a hydrogen rich stream, is an historical and industrially important reaction. After the development of the low temperature shift catalyst composed of copper and zinc oxide during the 1960s, the main application of the water gas shift reaction has been hydrogen production for ammonia synthesis or other industrial processes such as hydro treating of petroleum stocks. However, recently a new application for the water gas shift reaction is in reforming systems for fuel cells. In particular, research activity is growing in catalyst characterization, kinetic and reactor modeling and new catalyst formulation.

To design an efficient fuel reformer and to optimize its operating conditions, knowing the kinetics for steam reforming and water gas shift is critical. In most hydrocarbon processors, the water gas shift reactor is the biggest and heaviest component because the reaction is relatively slow compared to the other reactions and is inhibited at higher temperatures by thermodynamics. Therefore, reducing the size of the water gas shift reactor is an important issue. For fuel cell applications, a compact, efficient and reliable fuel processor is highly desirable. To design a compact fuel reformer system using process simulation and optimization, WGS reaction kinetics are a required and key component.

A number of rate expressions have been reported and tested to evaluate the water gas shift reaction rate for various catalysts [1]:

$$CO + H_2O \leftrightarrow CO_2 + H_2, \quad \Delta H^{\circ}_{298} = -41.1\,\text{kJ/mol} \quad (1)$$

Different mechanisms, various elementary reaction paths, and different rate determining steps and assumptions as to the active sites of the catalyst, create numerous rate expressions. These expressions can be successfully fit to specific experimental data. If the data is highly precise, the goodness of fit can help guide the choice of mechanism. For example, the rate expression of a large industrial WGS reactor operating at high temperature and pressure could be different from a small reactor in a methanol reformer for a PEM fuel cell. In our study, we focus on those conditions most likely in the WGS reaction for a medium scale methanol reformer using a Sud-Chemie $Cu/ZnO/Al_2O_3$ commercial catalyst.

Although numerous studies of the reaction kinetics and mechanism for the water gas shift reaction have been

* Corresponding author. Tel.: +1-610-758-4791; fax: +1-610-758-5057.
E-mail address: hgs0@lehigh.edu (H.G. Stenger).

0378-7753/$ – see front matter © 2003 Elsevier B.V. All rights reserved.
doi:10.1016/S0378-7753(03)00614-1

Nomenclature

A	constant
A_0	pre-exponential factor ($\mathrm{mol\,gcat^{-1}\,h^{-1}\,atm^{-2}}$)
E	activation energy (kJ/mol)
ΔH°_{298}	standard heat of reaction (kJ/mol)
i	number of data points
k	rate constant for the water gas shift reaction ($\mathrm{mol\,gcat^{-1}\,h^{-1}\,atm^{-2}}$)
k_1	rate constant of H_2O adsorption
k_2	rate constant of CO adsorption
k_{-1}, k_{-2}	rate constant of the reversible shift reaction
K, K_{eq}	equilibrium constant
K_P	equilibrium constant of water gas shift reaction
K_1	adsorption equilibrium constants for H_2O
K_2	adsorption equilibrium constants for CO
K_3	adsorption equilibrium constants for CO_2
K_4	adsorption equilibrium constants for H_2
m	concentration exponent of H_2O
n	concentration exponent of CO
$nc_{CO,i}$	calculated molar flow rate of CO at the reactor outlet (mol/h)
$ne_{CO,i}$	experimental molar flow rate of CO at the reactor outlet (mol/h)
P_{CO}	partial pressure of CO (atm)
P_{CO_2}	partial pressure of CO_2 (atm)
P_{H_2}	partial pressure of H_2 (atm)
P_{H_2O}	partial pressure of H_2O (atm)
r_{CO}	reaction rate of CO ($\mathrm{mol\,gcat^{-1}\,h^{-1}}$)
R	gas constant (J/mol K)
T	temperature (K)

Greek letter

β	factor of reversible reaction, $\beta = P_{H_2}P_{CO_2}/P_{CO}P_{H_2O}K_P$

reported during the past few decades, there are still disagreements and contradictory reports over the active site and the reaction mechanism. It is also apparent that there are two distinctly different kinetic mechanisms: the "adsorptive mechanism" (reaction (2)) and "regenerative mechanism" (reactions (3) and (4)):

$$H_2O + CO \rightarrow CO_{(ads)} + H_2O_{(ads)} \rightarrow [int^*] \rightarrow CO_{2(ads)} + H_{2(ads)} \rightarrow CO_2 + H_2 \quad (2)$$

$$H_2O + Red \rightarrow H_2 + Ox \quad (3)$$

$$CO + Ox \rightarrow CO_2 + Red \quad (4)$$

where Red represents a reduced site and Ox an oxidized site.

In the adsorptive mechanism, CO and H_2O adsorb on the catalyst surface and form an intermediate which results in desorbed hydrogen and CO_2. Many research groups have tried to prove the existence and form of the intermediates, such as the formate species through chemical trapping experiments, isotopic labeling, or IR spectroscopy [2–5]. The regenerative mechanism or redox mechanism is the cycling of two steps (reactions (3) and (4)). In the first step water adsorbs and dissociates on reduced sites of catalyst surface to produce hydrogen while oxidizing a site. In the following step CO is oxidized to CO_2 on this oxidized sites [6–8].

From these two mechanisms, a variety of rate expressions can be derived. From the adsorptive mechanism, Langmuir–Hinshelwood type rate expressions can be derived. The following rate expression is derived from Yang–Hougen table [9] when the surface reaction is assumed rate controlling:

$$r_{CO} = k\frac{P_{H_2O}P_{CO} - P_{H_2}P_{CO_2}/K_P}{(1 + K_1P_{CO} + K_2P_{H_2O} + K_3P_{CO_2} + K_4P_{H_2})^2} \quad (5)$$

The above rate expression has been tested using plant and laboratory data by several authors [10,11] who report that only the Langmuir–Hinshelwood model can accommodate all of the experimental data. Alternatively, single path reaction mechanism applied to the adsorptive mechanism results in the following expressions [12]:

$$r_{CO} = k\frac{P_{H_2O}P_{CO} - P_{H_2}P_{CO_2}/K_P}{1 + K_1P_{H_2O} + K_3P_{CO_2}} \quad (6)$$

For the redox mechanism, Shchibrya et al. derived the following rate expression and confirmed its validity using Cu-Zn-Cr catalysts [6]:

$$r_{CO} = k\frac{P_{H_2O}P_{CO} - P_{H_2}P_{CO_2}/K_P}{AP_{H_2O} + P_{CO}} \quad (7)$$

Other research groups also report the validity of this rate expression from the oxidation–reduction mechanism [13]. Using a CuO/ZnO catalyst, another rate expression can be derived from the redox mechanism when a single path reaction model is assumed [12]:

$$r_{CO} = \frac{k_1k_2(P_{H_2O}P_{CO} - P_{H_2}P_{CO_2}/K_P)}{k_1P_{H_2O} + k_2P_{CO} + (k_{1-} + k_{2-})P_{CO_2}} \quad (8)$$

In contrast to those rate expressions from detailed reactions, mechanisms and rate determining steps, there are simple empirical rate expressions which do not consider any mechanism. Moe [14] used a simple reversible rate expression for carbon monoxide conversion:

$$r_{CO} = k\left(P_{CO}P_{H_2O} - \frac{P_{CO_2}P_{H_2}}{K_P}\right) = kP_{CO}P_{H_2O}(1-\beta) \quad (9)$$

where

$$\beta = \frac{P_{CO_2}P_{H_2}}{P_{CO}P_{H_2O}K_{eq}}$$

Other research groups have reported that the water gas shift reaction is not a simple order reaction, especially at higher

steam/CO ratios, and have tried to find proper exponent parameters in a power-law type equation [15]:

$$r_{CO} = kP_{CO}^{n} P_{H_2O}^{m}(1-\beta) \quad (10)$$

The water gas shift reaction is an important reaction in the fuel reformer because of the reactor's size. It is important to include the effects of other reactions in the reforming system: hydrocarbon reforming and CO selective oxidation, when designing the WGS reactor. The goal of this study is to obtain highly accurate kinetics expressions for the WGS reaction to create a tool for an integrated and optimized simulation of a whole fuel processing system.

2. Experimental

For our experimental work we have chosen to use a commercial catalyst and reaction conditions similar to the reactor conditions of a fuel processor such as: feed gas composition, space velocity, pressure, and reactor temperature. The commercial catalyst used was $Cu/ZnO/Al_2O_3$ catalyst manufactured by Sud-Chemie (Catalyst no.: EX-2248). This catalyst is also good for methanol decomposition and reforming. Catalyst information and XPS analysis can be found in our previous paper [16]. The catalyst was ground and sieved to a particle diameter of 200–250 μm to eliminate internal diffusion resistance but allow good gas distribution.

All reaction tests were performed in a standard catalyst test unit. A stainless steel tubular reactor, 1/2 in. in diameter and 12 in. long was used for all reaction tests. To ensure isothermal conditions along the bed length, a split tubular furnace was used and the temperature of catalyst bed was measured directly by a 1/16 in. J-type thermocouple. The reaction tests were performed at temperatures between 120 and 250 °C. The water feed rates were controlled precisely by a syringe pump, 74900 Series (Cole Palmer), from 0.5 to 8 ml/h. To simulate the conditions exiting a methanol reforming unit, the feed gas stream was a 1:2 mixture of CO and H_2. The catalyst loading was 1.0 g and the GHSV at reaction temperature was controlled between 1000 and 20,000 h^{-1}.

The effluent of the reactor was maintained at 120 °C with heating tapes to avoid liquid condensation and connected directly to a CARLE Series S gas chromatograph, which uses a Hydrogen Transfer System (Pd membrane) for hydrogen analysis. This is a specially designed GC has two thermal conductivity detectors using two different carrier gases: helium and nitrogen. Helium is the preferred carrier gas for all components except hydrogen while nitrogen is the proper carrier gas for hydrogen. Two columns: Alltech Chemisorb 107 (80–100 mesh, 6 ft × 1/8 in.) and Supelco Carboxen 1000 (60–80 mesh, 15 ft × 1/8 in.) were connected in series to analyze the condensible and light gas components. Four components: water, H_2, CO, CO_2 were measured during each test run. Material balances on carbon were calculated to verify measurement accuracy, and for all runs reported here were within 3% of closure.

3. Results and discussion

3.1. Water gas shift reaction thermodynamics

From thermodynamic properties and relations the equilibrium constant for the water gas shift reaction can be derived in a conventional way as shown in the following equation [17]:

$$\ln(K_{eq}) = \frac{5693.5}{T} + 1.077 \ln T + 5.44 \times 10^{-4} T - 1.125 \times 10^{-7} T^2 - \frac{49170}{T^2} - 13.148 \quad (11)$$

where

$$K_{eq} \cong \frac{P_{CO_2} P_{H_2}}{P_{H_2O} P_{CO}}$$

a simpler equation for K_{eq} is given by Moe [14]:

$$K_{eq} = \exp\left(\frac{4577.8}{T} - 4.33\right) \quad (12)$$

According to the above equations, the equilibrium constant of water gas shift reaction is 210 at 200 °C and 38.8 at 300 °C. The water gas shift reaction is moderately exothermic reaction ($\Delta H^{\circ}_{298} = -41.1$ kJ/mol) and its equilibrium constant decreases with increasing temperature.

At a given temperature and thus a given equilibrium constant, and a given feed composition, equilibrium conversion of the WGS reaction can be calculated. Fig. 1 shows the calculated exiting CO concentration if a reactor reaches equilibrium conversion. According to this figure, reaching very low CO exiting concentrations requires very low temperatures and/or high water to CO ratios.

3.2. Water gas shift reaction data

Fig. 2 shows experimental measurements of carbon monoxide conversion versus H_2O/CO ratio over the temperature range of 120–250 °C. As expected the conversion of CO increases with increasing H_2O/CO ratio at constant temperature. For example, a 1:1 molar feed ratio and 220 °C, the conversion reaches 70%. The equilibrium conversion for these conditions is calculated as 87%. For approximately an equal-molar H_2O and CO mixture, the effect of space velocity was investigated (Fig. 3). The three isotherms in this figure show that as expected the conversion of the WGS reaction decreases slowly with increasing space velocity.

To determine the deactivation characteristics of the $Cu/ZnO/Al_2O_3$ catalyst for the WGS reaction, a durability test was performed for 250 h at various feed and operating conditions. For the case of methanol decomposition with this catalyst the activity decreased rapidly during the initial

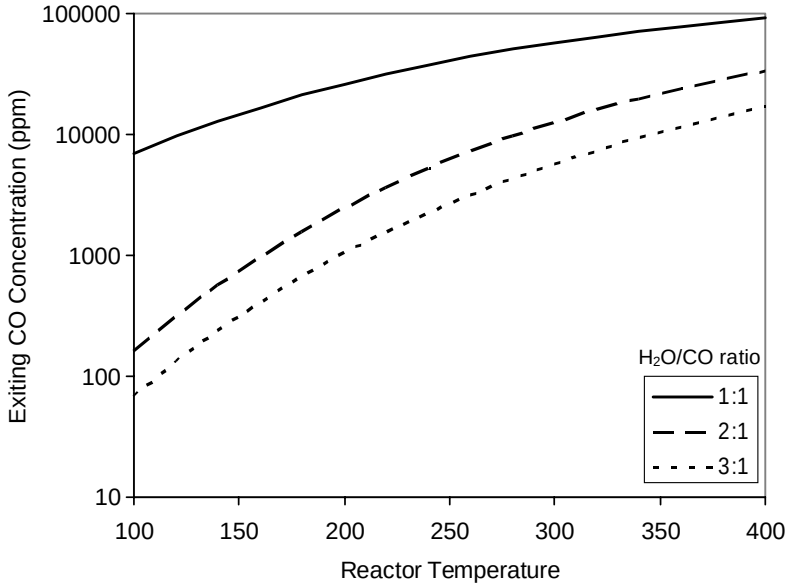

Fig. 1. CO exiting concentration for equilibrium conversion of water gas shift reaction with various inlet H_2O/CO mole ratios, 1 atm, feed $H_2/CO = 2.0$.

period of operation [16]. However, as shown in Fig. 4, there was no rapid initial decrease of the activity for the WGS reaction. The extent of activity loss for the WGS case was approximately 10% over 250 h while the activity of methanol decomposition dropped almost 25% during the first 10 h.

3.3. Kinetic studies and rate expressions

To find the most accurate rate expression for the water gas shift reaction, several kinetic models were selected to fit the experimental data of the 30 data sets shown in the Fig. 2. The rate expressions selected for the evaluation are listed in Table 1. The exiting molar flow rate of each reactant and product was determined by numerically integrating a one-dimensional isothermal PFR model. The constants in each model were assumed to be Arrhenius functions of temperature ($A_0 \exp(-E/RT)$).

To obtain the exiting concentration of the reactor, the MATLAB subroutine function ODE23 was used for numerical integration. To determine the kinetic parameters, the expression in Eq. (13) was minimized:

$$\text{minimize} \left\{ \sum_{i=1}^{N} (\text{ne}_{\text{CO},i} - \text{nc}_{\text{CO},i})^2 \right\} \tag{13}$$

where i is the experiment number ($N = 30$ for WGS); $\text{ne}_{\text{CO},i}$ the experimental molar flow rate of CO at the reactor outlet (mol/h); $\text{nc}_{\text{CO},i}$ the calculated molar flow rate of CO at the reactor outlet (mol/h).

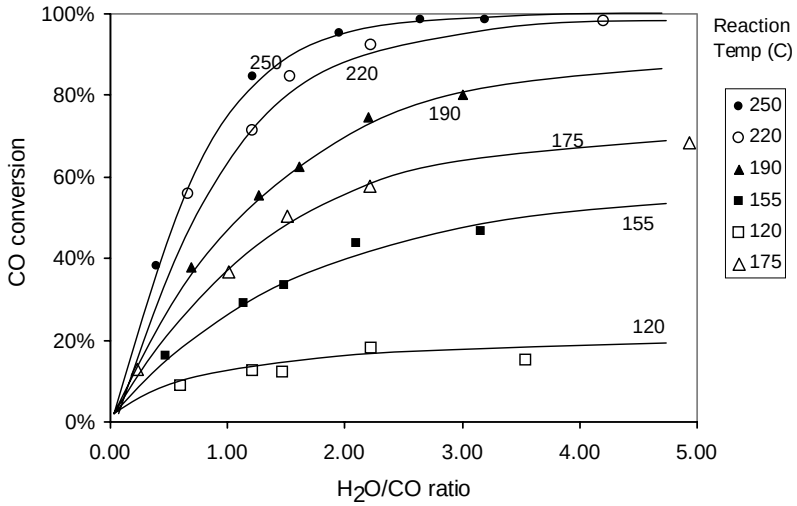

Fig. 2. Water gas shift reaction: CO conversion vs. H_2O/CO ratio (reaction temperature: 175–250 °C; catalyst loading: 1.0 g; pressure: 1 atm; GHSV: 6100 h^{-1}).

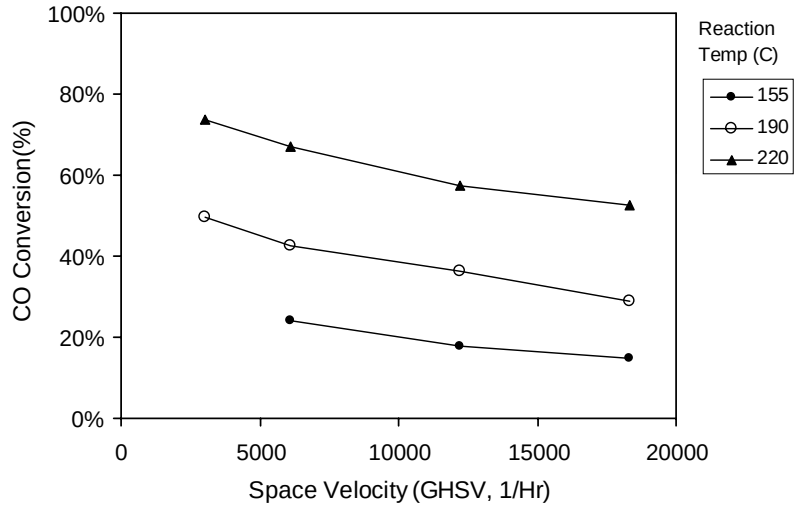

Fig. 3. Water gas shift reaction: CO conversion as a function of space velocity (reaction temperature: 155–220 °C; catalyst loading: 1.0 g; pressure: 1 atm; H_2O/CO: 1.18–1.33; GHSV: 3000–18,000 h^{-1}).

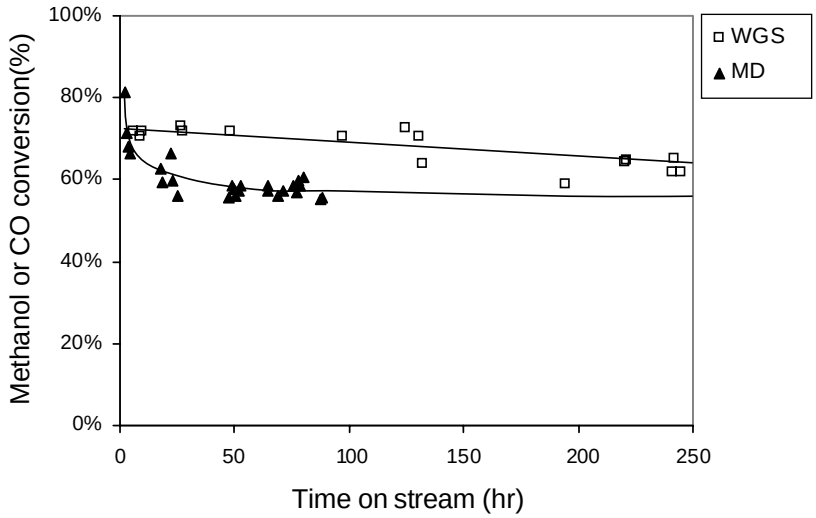

Fig. 4. Deactivation of catalyst for water gas shift reaction and methanol decomposition: (a) CO conversion vs. time on-stream (reaction temperature: 155–220 °C; H_2O/CO: 1.18–1.33; GHSV: 6100 h^{-1}); (b) methanol conversion vs. time on-stream (reaction temperature: 300 °C, GHSV: 1100 h^{-1}).

To find the parameters that minimized Eq. (13), the MATLAB subroutine function LSQNONLIN was used for non-linear least squares optimization.

The quality of the fit is demonstrated in Fig. 5 by comparing the observed and calculated CO exiting flow rates for all the experiments for models 4 and 5 of Table 1. Among the five rate expressions evaluated, model 4, the single path redox mechanism, fits the data best. Model 1, the double site Lanmuir–Hinshelwood type rate expression from the adsorptive mechanism also fits the experimental data very well.

Table 1
Evaluation of kinetic models from different mechanisms

Model	Type	Rate expression, r	NOP[a]	Dsq[b]	R	Reference
1	Adsorptive	$kP_1P_2(1-\beta)/(1+\sum_{i=1}^{4}K_iP_i)^2$	10	0.49	0.996	[9,10]
2	Adsorptive	$kP_1P_2(1-\beta)/(1+K_1P_1+K_3P_3)$	6	1.51	0.989	[12]
3	Regenerative	$kP_1P_2(1-\beta)/(P_1+AP_2)$	4	3.80	0.987	[6,13]
4	Regenerative	$k_1k_2P_1P_2(1-\beta)/(k_1P_1+k_2P_2+K_3P_1)$	6	0.56	0.996	[14]
5	Empirical	$kP_1P_2(1-\beta)$	2	1.79	0.986	[15]

P_1–P_4: partial pressure of CO, H_2O, CO_2, H_2.

[a] Number of parameters.

[b] $\text{Dsq} = \sum_{i=1}^{N}(\text{ne}_i - \text{nc}_i)^2$.

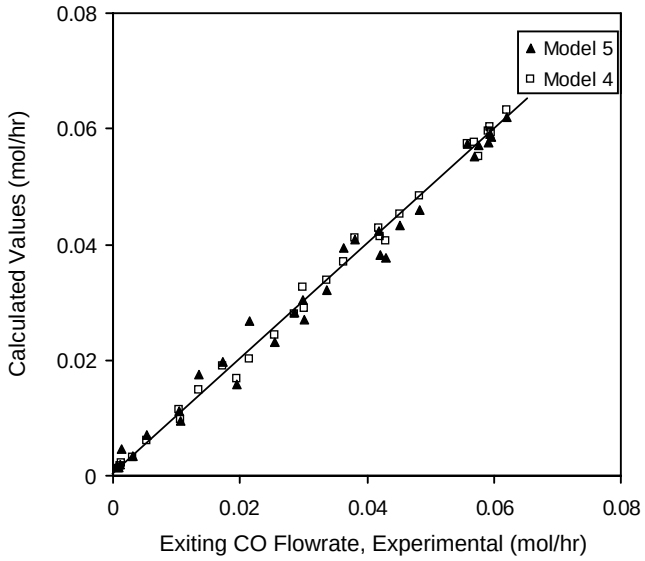

Fig. 5. Comparison of experimental exiting CO flow rate data with calculated numerical value using models 4 and 5 in Table 1 (temperature: 120–250 °C; catalyst loading: 1.0 g; pressure: 1 atm).

However, all five mechanisms gave very high R^2 values indicating that any of the models are adequate for simulation purposes.

The empirical rate expression derived from the numerical fitting is:

$$r_{CO} = 2.96\times10^5 \exp\left(-\frac{47400}{RT}\right)\left(P_{CO}P_{H_2O} - \frac{P_{CO_2}P_{H_2}}{K_e}\right) \quad (14)$$

The activation energy for the empirical model of 47.4 kJ/mol is consistent with other values in the literature. The comparison of activation energy and frequency factors with other first order rate expressions or empirical power-law equations are summarized in Table 2.

3.4. Simulation of the water gas shift reactor

The design of a water gas shift reactor used to generate fuel cell grade hydrogen must choose several operating parameters subject to several constraints. Five critical design constraints include (1) the inlet gas composition; (2) the inlet gas flow rate; (3) the temperature exiting the reforming reactor; (4) the exiting CO concentration constraint of the down stream processes; and (5) the water requirements for proper operation of the fuel cell. For the case of methanol steam reforming, the gas typically contains H_2 and CO in a ratio between 2 and 3, with some residual water. The exiting reformer temperature is near 300 °C, and the flow rate must be high enough to meet the fuel cell electrical output requirements, which is approximately 12 l of H_2/(min kW) of electrical output (Table 3). Exiting the WGS reactor, the CO concentration must be low enough to be fed directly to the fuel cell (about 50 ppm of CO), or more typically it must be moderately low so it can be treated by preferential oxidation (about 1 mol%). The water content should be near 12 mol% for proper humidification of a PEM fuel cell. The actual optimum water concentration depends on fuel cell operating pressure and temperature. The values of these constraints are somewhat flexible since the full optimization of the fuel cell design could include them as independent, not fixed variables.

Table 2
Parameter comparison for empirical expressions ($r = k_0 \exp(-E/RT) P_{CO}^m P_{H_2O}^n (1-\beta)$)

Catalyst	m	n	$\ln k_0$	E (kJ/mol)	Reference
ICI-Cu/ZnO/Al_2O_3	1	1	15.2	52.8	[15]
Cu/Al_2O_3	1	1.9	–	69.3	[8]
Cu/ZnO/Al_2O_3	0	1	–	41.8	[18]
CuO/MnO_2	1	1	–	55.0	[19]
Cu/ZnO/Al_2O_3	1	1	12.6	47.4	This work

Table 3
Design basis for WGS reactor simulation and 1 kW fuel cell

	Design variables	Values
WGS reactor	CO inlet molar flow rate (gmol/h)	11.1
	H_2 inlet molar flow rate (gmol/h)	22.2
	CO target conditions (mol%)	1
Fuel processor	Required amount of hydrogen (gmol/h)	33.3
		12.4[a]
Fuel cell stack	Target power (kW)	1
	Stack voltage, 50 cells (V)	35
	Cell amperage (A)	28.57
	Fuel cell efficiency, assumed (%)	80

[a] The unit of the value is slpm.

The WGS reactor design parameters used to meet these constraints include (1) reactor temperature; (2) water addition rate; and (3) reactor size (weight of catalyst). This multi constrained, three-dimensional problem lends itself to simulation for analysis, because the tradeoffs between the parameters are not obvious.

For simulation and analysis, an electrical generating capacity of 1 kW is chosen, and methanol is chosen as the reformer feed. The basis for this fuel cell is summarized in the Table 3. The simulation uses the empirical kinetic model shown in Eq. (14) because of its accuracy and simplicity. It also assumes no mass or heat transfer resistance and it assumes the reactor is plug flow and isothermal. Although these assumptions are not entirely correct, they allow observation of the general reactor behavior.

Fig. 6 is a contour plot of the variable space needed (reactor temperature, catalyst weight, and feed water rate) to meet the conditions of 1 mol% CO exiting the WGS reactor. Fig. 7 plots results from the same set of simulations as in Fig. 6, except the vertical axis is the water concentration leaving the WGS reactor. Due to kinetic limi-

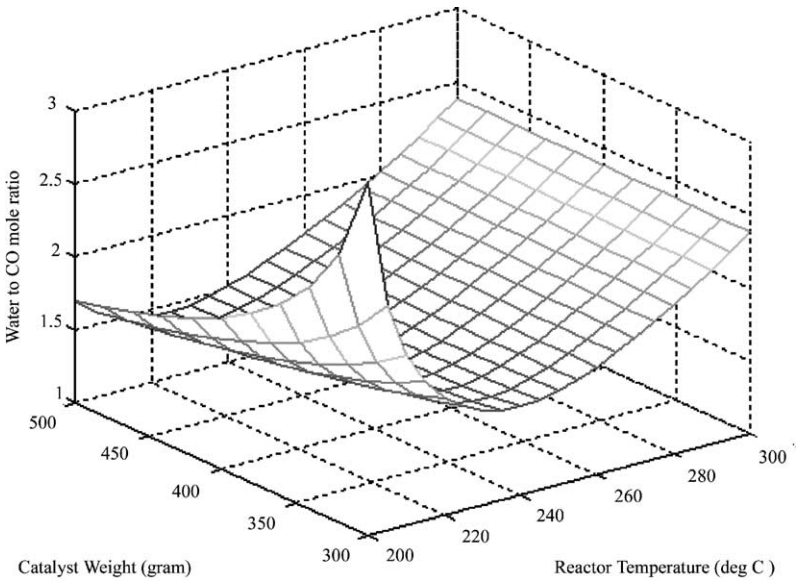

Fig. 6. Simulation result of water gas shift reactor for 1 kW fuel cell: required water amount to achieve 1 mol% of exiting CO concentration according to various temperature and catalyst loading (temperature: 200–300 °C; CO inlet: 11.1 mol/h; pressure: 1 atm).

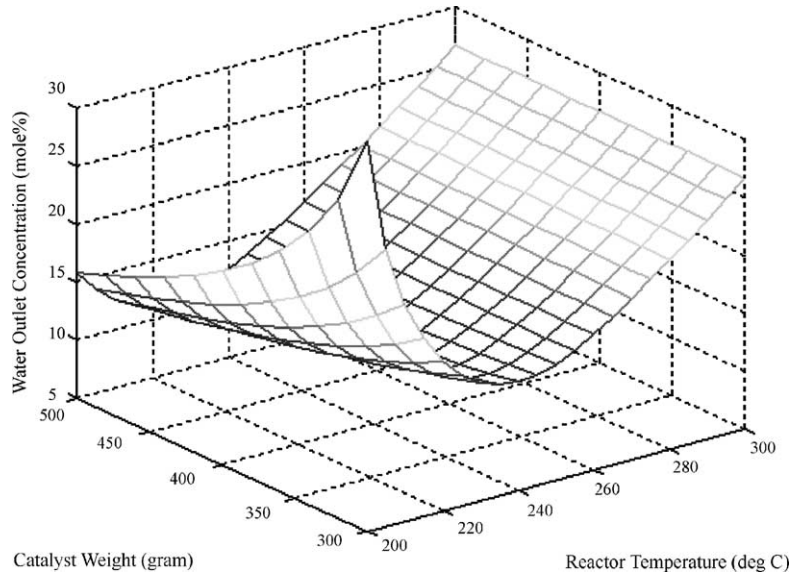

Fig. 7. Simulation result of water gas shift reactor for 1 kW fuel cell: water outlet concentration to achieve 1 mol% of exiting CO concentration according to various temperature and catalyst loading (temperature: 200–300 °C; CO inlet: 11.1 mol/h; pressure: 1 atm).

tations, these figures show a steep increase in water required and water exiting at low temperatures and low catalyst loadings. Due to equilibrium constraints, they show a slow increase in water exiting and water required at higher temperatures. A major concern for fuel cell operation is to maintain the proper water concentration in the feed gas. This suggests it may be optimal from a control perspective, to operate the WGS reactor at a temperature where the water concentration variation is small for a given perturbation in feed composition, temperature or space velocity. For this catalyst that temperature would be at the bottom of the valley in Figs. 6 and 7, or near a temperature of 230–240 °C.

4. Conclusions

Several kinetic rate expressions can adequately model the water gas shift reaction over the $Cu/ZnO/Al_2O_3$ catalyst used in this study. Two rate expressions, one derived from an adsorptive mechanism and one from a redox mechanism, were found to be the most accurate models. However, even

an empirical rate expression (Eq. (14)) was found to fit the data with a high degree of accuracy.

Applying the empirical kinetic relationship in a simple isothermal plug flow model shows that to maintain a constant CO and water concentration exiting the reactor requires controlling the reactor temperature and the water addition rate closely. These two exiting compositions are important to maintain steady operation of the fuel cell. Large variations in CO concentration will make downstream oxidation of CO more difficult to control, resulting in fluctuating CO concentrations entering the fuel cell, which will result in fluctuating current and voltages. Large variations in water exiting the WGS reactor will make controlling the moisture needed for proper PEM operation more difficult.

The results of this study are expected to be an important component for the overall design, optimization and control of commercial fuel reformers used to generate hydrogen for fuel cells.

Acknowledgements

The authors thank the Air Pollution Educational and Research Grant (APERG) Scholarship Program from Mid-Atlantic States Section, Air & Waste Management Association (MASS-AWMA).

References

[1] M.V. Twigg, Catalyst Handbook, second ed., 1989, pp. 283–339.
[2] T.M. Yureva, Kinet. Katal. 10 (1969) 862.
[3] C. Rhodes, G.J. Hutchings, A.M. Ward, Catal. Today 23 (1995) 43–58.
[4] T. Shido, Y. Iwasawa, J. Catal. 129 (1991) 343–345.
[5] G.J. Millar, C.H. Rochester, K.C. Waugh, J. Catal. 142 (1993) 263–273.
[6] G. Shchibrya, N. Morozov, M. Temkin, Kinet. Catal. USSR 6 (1965) 1010.
[7] O. Jakdetchai, T. Nakajima, J. Mol. Struct. (Theor.) 619 (2002) 51–58.
[8] C.V. Ovesen, et al., J. Catal. 158 (1996) 170–180.
[9] G.F. Froment, K.B. Bischoff, Chemical Reactor Analysis and Design, second ed., Wiley, New York, 1990.
[10] J.S. Cambell, Ind. Eng. Chem. Proc. Res. Dev. 9 (1970) 588.
[11] N. Amadeo, M. Laborde, Int. J. Hydrogen Energy 20 (12) (1995) 949–956.
[12] E. Fiolitakis, H. Hofmann, J. Catal. 80 (1983) 328–339.
[13] D. Newsome, Catal. Rev. Sci. Eng. 21 (2) (1980) 275–318.
[14] J.M. Moe, Chem. Eng. Pro. 58 (1962) 33.
[15] R.L. Keiski, O. Desponds, Y.F. Chang, G.A. Somorjai, Appl. Catal. A 101 (1993) 317–338.
[16] Y. Choi, H.G. Stenger, Appl. Catal. B: Environ. 38 (2002) 251–361.
[17] G.C. Chinchen, P.J. Denny, J.R. Jennings, M.S. Spencer, K.C. Waugh, Appl. Catal. 36 (1988) 1–65.
[18] M.J.L. Gines, N. Amadeo, M. Laborde, C.R. Apesteguia, Appl. Catal. A: Gen. 131 (1995) 283–296.
[19] G.J. Hutchings, et al., J. Catal. 137 (1992) 408–422.